Free Radical Biology and Medicine 85 (2015) 114–126

Contents lists available at ScienceDirect

Free Radical Biology and Medicine

journal homepage: www.elsevier.com/locate/freeradbiomed

Original Contribution

# Novel mechanisms for superoxide-scavenging activity of human manganese superoxide dismutase determined by the K68 key acetylation site

Jiaqi Lu [a,1], Kuoyuan Cheng [a,1], Bo Zhang [a], Huan Xu [a], Yuanzhao Cao [a], Fei Guo [a], Xudong Feng [b,*], Qing Xia [a,*]

[a] State Key Laboratory of Natural and Biomimetic Drugs, Department of Chemical Biology, School of Pharmaceutical Sciences, Peking University, Beijing, People's Republic of China

[b] Department of Medicine, Children's Hospital Boston, Harvard Medical School, Boston, MA 02445, USA

ARTICLE INFO

*Article history:*
Received 2 October 2014
Received in revised form
22 March 2015
Accepted 9 April 2015
Available online 20 April 2015

*Keywords:*
Superoxide
Superoxide dismutase
Acetylation
ROS
Mitochondria
Structure
Electrostatic potential
Tetramerization

ABSTRACT

Superoxide is the primary reactive oxygen species generated in the mitochondria. Manganese superoxide dismutase (SOD2) is the major enzymatic superoxide scavenger present in the mitochondrial matrix and one of the most crucial reactive oxygen species-scavenging enzymes in the cell. SOD2 is activated by sirtuin 3 (SIRT3) through $NAD^+$-dependent deacetylation. However, the exact acetylation sites of SOD2 are ambiguous and the mechanisms underlying the deacetylation-mediated SOD2 activation largely remain unknown. We are the first to characterize SOD2 mutants of the acetylation sites by investigating the relative enzymatic activity, structures, and electrostatic potential of SOD2 in this study. These SOD2 mutations affected the superoxide-scavenging activity in vitro and in HEK293T cells. The lysine 68 (K68) site is the most important acetylation site contributing to SOD2 activation and plays a role in cell survival after paraquat treatment. The molecular basis underlying the regulation of SOD2 activity by K68 was investigated in detail. Molecular dynamics simulations revealed that K68 mutations induced a conformational shift of residues located in the active center of SOD2 and altered the charge distribution on the SOD2 surface. Thus, the entry of the superoxide anion into the coordinated core of SOD2 was inhibited. Our results provide a novel mechanistic insight, whereby SOD2 acetylation affects the structure and charge distribution of SOD2, its tetramerization, and p53–SOD2 interactions of SOD2 in the mitochondria, which may play a role in nuclear–mitochondrial communication during aging.



## 1. Introduction

In mammalian cells, the mitochondrion is the major site of adenosine triphosphate production and a vital site for other diverse cellular functions, including metabolism, generation of reactive oxygen species (ROS)[2], stress response, and apoptosis [1–3]. Despite ongoing controversies, theoretically, the mitochondrion has been regarded as the biological clock for aging [4]. The imbalance between mitochondrial ROS production and antioxidant capacities underlies many oxidative stress- and age-related diseases, including neurodegenerative diseases, atherosclerosis, carcinogenesis, and diabetes [2,5–7]. The superoxide anion $O_2^{\bullet -}$ is the primary ROS produced by complexes I and III of the electron transport chain in the mitochondrion. $O_2^{\bullet -}$ is one of the toxic oxygen radicals that could further lead to formation of other oxidative species, such as hydrogen peroxide ($H_2O_2$), hydroxyl radical, and peroxynitrite ($OONO^-$), which inflict damage on both the mitochondria and the cell. In the mitochondrial matrix, the steady-state concentration of $O_2^{\bullet -}$ may be estimated to be as low as $10^{-10}$ M [8], which is believed to be maintained by the scavenging enzymes within the mitochondria, such as superoxide dismutase (SOD) and/or superoxide reductase [9]. However, Wang et al. [10] indicated that the mitochondria undergo bursts of superoxide production at a single mitochondrial level, which is called "superoxide flash," signifying the fluctuating concentrations of the superoxide molecules in the mitochondria. Among all the ROS-scavenging enzymes in the mitochondria, manganese superoxide dismutase (SOD2 or MnSOD) is the pivotal antioxidant enzyme that

*Abbreviations:* SOD2, manganese superoxide dismutase; ROS, reactive oxygen species; MD, molecular dynamics; PTM, posttranslational modification; Anh, acetic anhydride; MnTM-4-PyP, manganese(III) *meso*-tetrakis (*N*-methylpyridinium-4-yl) porphyrin.

* Corresponding authors.
*E-mail addresses:* xudong.feng@childrens.harvard.edu (X. Feng), xqing@hsc.pku.edu.cn (Q. Xia).

[1] These authors contributed equally to this work.

http://dx.doi.org/10.1016/j.freeradbiomed.2015.04.011
0891-5849/

catalyzes the dismutation of superoxide radicals to hydrogen peroxide and molecular oxygen, protecting cells from oxidative stress. The intramitochondrial level of SOD2 is believed to be 10 to 40 μM. This dismutation reaction is considered to be fast, similar to diffusion ($k = 2.3 \times 10^9\ M^{-1}\ s^{-1}$), indicating that this reaction is catalyzed by a highly effective superoxide dismutase [8]. In various studies, many investigators have characterized different SOD2 mutants to illustrate the biological function and structure–activity relationship of SOD2; however, nobody has acquired a mutant with activity higher than that of wild-type SOD2 [11–15]. In recent years, several studies have reported that the antioxidative activity of the SOD2 is regulated by many posttranslational modifications (PTMs), including acetylation [16,17], methylation [18], phosphorylation [19], nitration [14,20], and glutathionylation [20]. These explorations have provided new methods to possibly obtain a higher-activity mutant form of SOD2 by changing the PTMs in SOD2.

Lysine acetylation has emerged as a key regulatory mechanism of protein function in diverse biological processes, including histone degradation [21], chromatin remodeling, transcription, and metabolism pathways in the mitochondria [22]. Compared with cytosol, the mitochondrion is a preferable environment for the acetylation reaction because of the higher concentration of acetyl-CoA (3- to 50-fold that of cytosol), which provides the acetyl group for acetylation, and the high pH (pH 8.0) [23], at which the nonenzymatic process of acetylation may occur. Recently, large-scale proteomic approaches have identified numerous mitochondrial acetylated proteins in both humans and mice [24–26], of which many are the enzymes involved in the intermediary metabolic processes, including fatty acid metabolism, urea cycle, tricarboxylic acid cycle, and gluconeogenesis. According to Xiong and Guan, these metabolic enzymes are affected by acetylation in a coordinated manner through various mechanisms, such as inhibition, activation, and protein destabilization [27]. Meanwhile, the cross talk between acetylation and phosphorylation/methylation regulates the key enzymes of the metabolism in response to different physiological stimulations [28]. SOD2 functions as the first responsive enzyme in the mitochondria to cope with the surge of superoxide molecules and is activated by deacetylation of specific lysine (K) residues, including K53, K68, K89, K122, and K130, which are identified in both humans and mice by mass spectrometry [17,29–31]. As shown in Fig. 1, these lysine residues (marked red) are conserved among various species, including yeast, *Drosophila*, mouse, rat, and bovine. One intriguing problem is that the acetylation sites identified in SOD2 in humans are different from those in mice; for instance, K122 is the acetylation site in mice, whereas K68 is the acetylation site in humans [30]. The deacetylation of these lysine residues in SOD2 is catalyzed by SIRT3 [30], a mitochondrial deacetylase [32] of the sirtuin family that functions in the regulation of antioxidative responses [33–35]. Although the deacetylation-mediated SOD2 activation seems to be clearly illustrated in the aforementioned studies, the mechanism underlying this activation by which the acetylation site exactly determines the SOD2 activity in humans and whether there may exist any unknown sites that are also involved in SIRT3-mediated deacetylation of SOD2 remain to be elucidated. Meanwhile, the mechanism underlying the acetylation-dependent SOD2 activity remains unclear. To answer these questions, one explanation that is consistent with the model proposed by Fridovich et al. in 1983 [36] indicated that deacetylation of lysine residues could form a cationic region to attract the negatively charged superoxide molecules, which increases the SOD2 activity [37]. However, more experiments are needed to demonstrate the existence of such a mechanism. In this study, we aimed to further investigate the SOD2 acetylation mechanisms. By applying the novel method of nonenzymatic covalent conjugation to add acetyl groups to lysine residues, we confirmed that lysine acetylation decreased the SOD2 activity in vitro. We identified more potential acetylation sites, such as K154 and K194, in SOD2. In addition, we investigated the details of the contributions of each of these lysine residues to SOD2 acetylation and activity in HEK293T cells. In this work, we highlighted K68 as the most important among the investigated acetylation sites in modulation of SOD2 activity in human cells. We also studied the mechanism by which the acetylation of these lysine residues affects the SOD2 activity. Through molecular dynamic simulations, we revealed that K68 mutations could cause significant conformational changes in the coordinated active core and alter the entire charge distribution of SOD2. We found that these mutations also affected the tetramer stability and protein–protein interactions of SOD2. These findings imply a novel function of lysine acetylation in SOD2 that is important for the enzymatic activity of SOD2 and disturbs the overall SOD2 structure and tetramerization. Thus, the endogenous SOD2 activity in human cells is regulated in a combined manner.

## 2. Materials and methods

### 2.1. Protein expression, purification, and site-directed mutagenesis

For protein expression in *Escherichia coli*, full-length SOD2 cDNA was subcloned into the pET26b(+) vector and the plasmid was transformed into BL21(DE)3 competent cells. Bacterial cells were grown in Luria–Bertani broth containing 50 μg/ml kanamycin. Isopropyl β-D-1-thiogalactopyranoside (0.6 mM) was added when the $OD_{600}$ reached 0.6. The expression of His-tagged SOD2 was induced at 16 °C overnight. The *E. coli* cells were then collected and lysed with

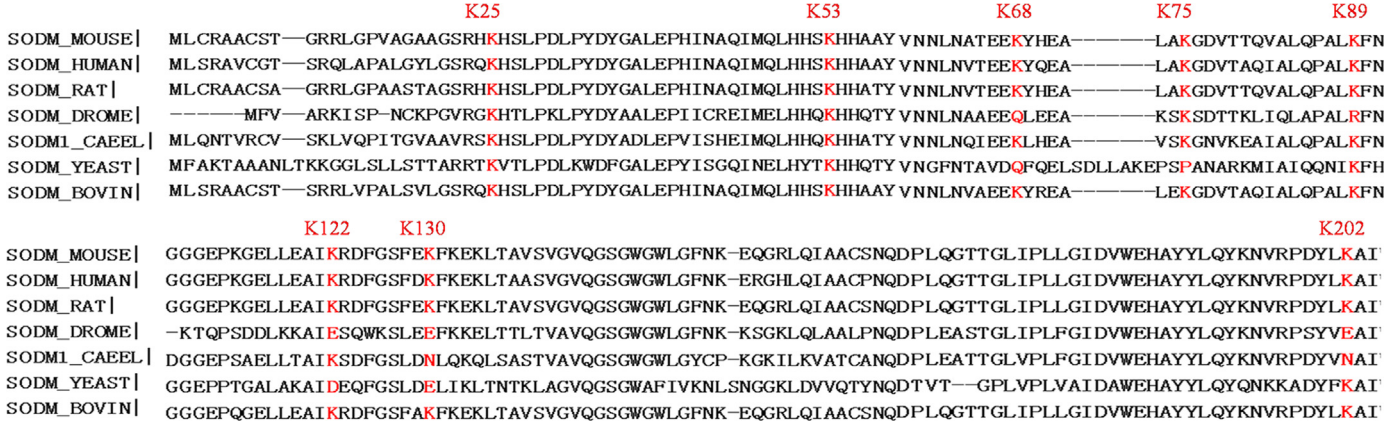


**Fig. 1.** The sequence alignment of SOD2 from various species. SOD2 sequences from various species were aligned and acetylated lysines that have been reported in mouse and human are marked red. DROME refers to *Drosophila melanogaster*, and CAEEL refers to *Caenorhabditis elegans*.

lysozyme and the supernatant was incubated with Ni-NTA agarose (Novagen), washed with 50 mM imidazole buffer four times, and eluted with 500 mM imidazole. Sodium dodecyl sulfate polyacrylamide gel electrophoresis (SDS–PAGE) was performed to test the purity. The concentration of purified proteins was determined with the BCA assay and equal amounts of wild-type and lysine mutants were subjected to inductively coupled plasma–mass spectrometry (ICP–MS) analysis to test the manganese concentration. For their expression in HEK293T cells, pCMV6-SOD2-Myc-DDK (Origene) expression vectors carrying human SOD2 cDNAs with wild-type and lysine mutations were transfected into HEK293T cells using Megatran 1.0. HEK293T cells were cultured in Dulbecco's modified Eagle's medium containing 10% fetal bovine serum at 37 °C and 5% $CO_2$. The cells described above were lysed in RIPA lysis buffer supplemented with complete protease inhibitor cocktail (Roche) and cell debris was removed by centrifugation at 13,000 rpm for 20 min. The concentrations of proteins from the lysate were quantified by BCA assay. The expression level of SOD2 protein was measured using Western blotting with anti-c-myc and anti-SOD2 antibodies (Santa Cruz Biotechnology, Santa Cruz, CA, USA). A QuickChange Lightning Site-Directed Mutagenesis Kit (Stratagene) was used to mutate lysine residues at positions 25, 53, 68, and 122 of SOD2 to glutamine, alanine, or arginine, respectively.

### 2.2. Measurement of SOD activity

SOD activity was measured with the WST-1 assay. Purified SOD2 protein and the mutant proteins were diluted in phosphate-buffered saline to the final concentration of 0.01 mg/ml, and 20 μl of protein solution was added to the reaction system containing superoxide generated by xanthine oxidase, and the inhibition rate of the oxidation of WST-1 formazan was measured with kits (Beyotime) according to the manufacturer's protocol. For measurement of total SOD activity in cellular homogenates, cell lysates in RIPA buffer were diluted to the final concentration of 0.50 mg/ml, and 20 μl of lysates was added to the reaction system. To measure the SOD2 activity, the cell lysates were incubated with 5 mM NaCN to inhibit SOD1 activity before addition to the reaction system. SOD1 activity was obtained by subtracting SOD2 activity from total SOD activity.

### 2.3. Chemical acetylation and deacetylation reaction in vitro

Purified SOD2 protein was ultrafiltered in potassium phosphate buffer (pH 8.0) four times until the imidazole concentration was much lower. SOD2 at 2.5 mg/ml and acetic anhydride at 150 μM (Sigma, St. Louis, MO, USA) were mixed together (1:1) and the mixed solution was incubated at room temperature for 1 h. Tris–HCl (pH 8.0, 50 mM) was the added to quench the acetylation reaction.

### 2.4. Analyses of acetylated SOD2 and acetylated SOD2 mutants with mass spectrometry

For the MS analysis of chemically acetylated SOD2, 500 ng of acetylated or nonacetylated SOD2 was separated by SDS–PAGE and stained with Coomassie blue. The Coomassie blue-stained SOD2 protein bands were excised from the gel and the SOD2 protein-containing gel slices were digested with trypsin, subjected to tandem mass spectrometry, and analyzed by OrbiTrap analyzer. For MS analysis of the SOD2 expressed in HEK293T cells, 0.4 μM trichostatin A and 10 mM nicotinamide were added to the culture medium 12 h before harvest. Total cellular protein extracts prepared from HEK293T treated with or without MnTM-4-PyP were resolved using gel electrophoresis.

### 2.5. Western blot analysis

The samples were prepared following the protocols of protein expression and extraction described above. Twenty micrograms of total protein from each sample in loading buffer was boiled and separated by 12% SDS–PAGE and electroblotted onto a polyvinylidene difluoride membrane. The membrane was blocked with 5% nonfat milk in TBST (50 mM Tris–HCl, 150 mM NaCl, and 0.02% Tween 20, pH 7.5) at room temperature for 1 h and then incubated with rabbit/mouse polyclonal antibodies overnight at 4 °C. Anti-c-myc antibodies (1:2000, Santa Cruz Technology); anti-acetyllysine, anti-SIRT3, and anti-p53 antibodies (1:1000, Cell Signal Technologies); or anti-SOD2 antibodies (1:2000, Santa Cruz Technology) were diluted in TBST containing 5% defatted milk. The membranes were rinsed three times, each time for 10 min with TBST, followed by incubation with horseradish peroxidase-conjugated goat anti-rabbit/mouse IgG (1:5000) at room temperature for 1 h. After another three rinses with TBST as above, the protein bands were developed by an enhanced chemiluminescence detection kit (Millipore). The optical bands were visualized in a Fuji LAS-3000 dark box (FujiFilm Systems, Stamford, CT, USA) and band densities were quantified using Quantity One Analysis software.

### 2.6. Immunoprecipitation assay

Immunoprecipitation was performed by following the manufacturer's supplied protocol (Direct IP from Pierce Chemical Co., Rockford, IL, USA). Proteins from cells were extracted in lysis buffer (50 mM Tris–Cl, pH 7.5, 150 mM NaCl, 10% glycerol, 2 mM $MgCl_2$, 1 mM dithiothreitol, and 1% NP-40) supplemented with a Complete protease inhibitor cocktail (Roche). Protein extracts were subjected to centrifugation at 14,000 rpm for 10 min. Protein lysates were precleared with protein A/G magnetic beads (Pierce) for 30 min before immunoprecipitation with c-myc antibodies at 4 °C for 1 h or overnight. Immunoprecipitates were extensively washed with lysis buffer and eluted with 100 mM glycine, pH 3.0. SOD2 antibody and c-myc antibody were obtained from Santa Cruz Biotechnology.

### 2.7. Measurement of mitochondrial superoxide levels with flow cytometry assays

Superoxide production was determined by measuring oxidation of MitoSOX (5 μM; Invitrogen, Grand Island, NY, USA) in cells, following the manufacturer's instructions. HEK293T cells were cultured and stimulated by 50 μM antimycin A for 1 h and incubated for 10 min at 37 °C before being trypsinized, resuspended, and measured by flow cytometry (510 nm excitation/590 nm emission), and a minimum of 30,000 cells were counted for each sample. Results were from at least three separate experiments. Data are presented as the average ± SD. Probabilities were calculated using the *t* test. Mean fluorescence intensity was calculated using Cyto5.3 software (Tree Star, Ashland, OR, USA). Autofluorescence of cells was used for background correction and fold change was calculated relative to control.

### 2.8. Cell survival assay

Cells (250,000) were incubated with 200 μM paraquat (Accu Standard, New Haven, CT, USA) for 48 h [18]. Remaining adherent cells were trypsinized and counted using a cell counter. Results shown are from at least three separate experiments.

### 2.9. Molecular dynamics simulations

Molecular dynamics (MD) simulation was performed using the Amber11 simulation package. The crystallographic coordinates of the human SOD2 structure (Protein Data Bank (PDB) 2ADQ) were obtained from the RCSB Protein Data Bank. 2ADQ and K68A-2ADQ, K122Q-2ADQ, and K53Q-2ADQ were placed in an octahedral water box. $Cl^-$ counterions were added to neutralize the system electrically. The ff99SB force field was used for protein, Gaff force field was used for Mn, and TIP3P force field was used for water. A two-stage approach was applied to minimize the energy of the simulation systems. First, the protein was fixed and the water and ions were energy minimized. Then the entire system was energy minimized. A 20-ps MD simulation at constant volume was performed to heat the system to 300 K, and temperature was controlled to make the collision frequency 1.0 $ps^{-1}$. Then with a time step of 2 fs, the system was simulated at a constant temperature of 300 K and a constant pressure of 1 atm with a time constant of 1 ps. The simulation has a length of 10 ns. Statistical analyses were performed using the last 10 ns of simulation, during which the backbone root mean square deviation was stable.

### 2.10. Statistical analysis

Data are presented as the mean ± SEM. Statistical significance for multiple comparisons was determined by Student's *t* test or using the one-way analysis of variance with Tukey's honestly significant difference test (SPSS version 18.0). A probability of $P < 0.05$ was considered statistically significant.

## 3. Results

### 3.1. Chemical acetylation decreased SOD2 activity in vitro and the relative SOD2 activity was changed by the K68 and K122 mutations

SOD2 activity can be regulated through lysine acetylation. The deacetylation of lysine residues such as K68 and K122 in SOD2 increases SOD2 activity. Thus, we prepared the acetylated form of SOD2 and studied how its activity is changed with acetylation and deacetylation. We expressed wild-type (wt) SOD2 and its mutants, including K68Q, K68A, K68R, K122Q, and K122R, in *E. coli* and subsequently purified them to >95% purity. We then acetylated wtSOD2 with acetic anhydride (Anh) and analyzed the acetylated SOD2 by mass spectrometry. The results showed that 10 lysine residues in SOD2 were all chemically acetylated (Supplementary Table 1). Among these sites, we first discovered that K25, K75, K154, and K194 of SOD2 could be modified with the acetyl group and speculated that the deacetylation of these acetylated lysine sites in vivo would also activate SOD2. Furthermore, we detected the acetylation of K53 and K68 in the peptides of wtSOD2 without Anh treatment (Table 1), suggesting that these sites are acetylated in a physiological state. Western blots (Fig. 2A) showed that Anh treatment could increase the total level of acetyllysine when normalized to the SOD2 expression level. Moreover, the acetylated SOD2 activity was sixfold lower than that of the nonchemically acetylated SOD2 (Fig. 2B). We speculated that the sixfold change was caused by acetylation at multiple lysine residues as shown in Supplementary Table 2. We also measured the activities of SOD2 mutants, including K68Q, K68A, and K68R, through the WST-1 assay. The results are presented in Fig. 2C, which shows that all the mutants exhibited activities lower than that of wtSOD2 and that K68R exhibited activity significantly higher than those of K68Q and K68A. However, for the K122 mutants, no significant difference in SOD activity was observed between K122Q and K122R (Fig. 2C). To determine whether these enzymes were equally metallated, we conducted ICP–MS analysis on wtSOD2 and its mutants. The results showed that manganese concentrations were similar among all the enzymes examined (Supplementary Table 1).

### 3.2. Mutations of SOD2 acetylation sites altered the superoxide-scavenging activity and K68 was the main acetylation site contributing to the overall SOD2 activity

To further investigate which sites contribute the major role to SOD2 acetylation among all the lysine residues in SOD2, we introduced glutamine (Q), alanine (A), or arginine (R) substitution at the K25 (with the nonacetylated site as the control), K53, K68, and K122 sites, which are located close to the active center and have already been identified in MS data [18,30]. Substitution of lysine with glutamine mimicked the acetylated amino acid state as indicated by their similar charges and structures, whereas substitution with arginine mimicked the deacetylated state, which retained the positive charge of lysine. In addition, the substitution of alanine shortened the side chains of these lysine residues and removed the positive charge at these positions. The relative expression levels of the SOD2 mutants with glutamine substitution in the HEK293T cells were measured using Western blot, and the overall acetylated level of each mutant was detected using the pan-acetyllysine antibody (Fig. 3A). The results showed that K68Q and K122Q substitutions significantly decreased the overall acetylated level of SOD2, whereas K53Q substitution only slightly reduced the SOD2 acetylation level, which was in accordance with the previous results, indicating that K68 and K122 could be the important acetylation sites in SOD2. To study whether substitutions of these acetylation sites affect the SOD2 activity in HEK293T cells, we measured the relative SOD2 activity of various SOD2 mutants by monitoring the mitochondrial superoxide level in HEK293T. According to the fluorescence of MitoSOX, the mitochondrial superoxide indicator, these SOD2 mutants showed superoxide-scavenging activities significantly lower than that of the wtSOD2. In addition, among all the glutamine substitutions of these acetylation sites, K68Q displayed the lowest activity in HEK293T (62% of wild-type activity), whereas K53Q and K122Q showed only a moderately reduced SOD2 activity (85 and 82% of wt activity, respectively). Moreover, the importance of K68 was highlighted by the dramatic loss of activity in the K68A and K68Q mutants (73 and 61% increase in mitochondrial superoxide level, respectively) compared with the K122Q and K53Q mutants (21.5 and 22% increase in mitochondrial superoxide level, respectively; Fig. 3B). Correspondingly, we tested the total SOD activity, including both SOD1 activity and SOD2 activity, in the cell homogenates containing the various SOD2 mutants (Figs. 3C and 3D). No significant changes in SOD1 activity were found in these mutants (Fig. 3C), whereas SOD2 activity was significantly increased in the group overexpressing wtSOD2 and

**Table 1**
Posttranslational modifications of human SOD2 identified by MS.

| Position | Target | Modification | Classification | Highest peptide confidence | Sequence motif |
|---|---|---|---|---|---|
| 53 | K | Acetyl, methyl | Posttranslational | High | MQLHHSkHHAAYV |
| 68 | K | Acetyl, methyl | Posttranslational | High | LNVTEEkYQEALA |

Human wtSOD2 was expressed in *E. coli*, purified, and subjected to LTQ (Linear Ion Trap) Orbitrap XL–MS analysis. Methylation and acetylation of K53 and K68 were identified.

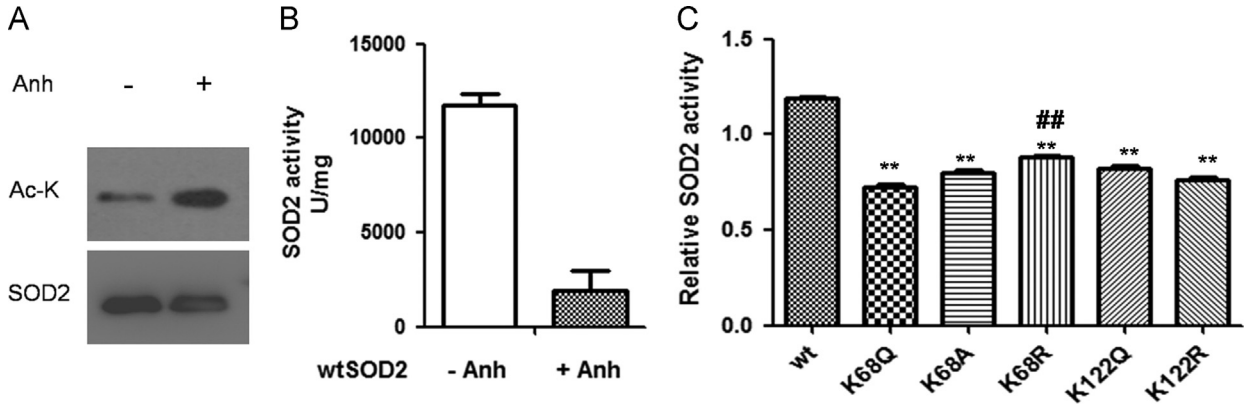


**Fig. 2.** Chemical acetylation decreased SOD2 activity in vitro and relative SOD2 activity was changed by mutations of K68 and K122. (A) 2.5 mg/ml human SOD2 and 150 μM acetic anhydride (Anh; Sigma) were mixed together (1:1) and incubated at room temperature for 1 h. The equal amounts of SOD2 treated with or without Anh were subjected to Western blot. (B) Superoxide-scavenging activity of human SOD2 treated with or without Anh was measured with WST-1 assay. $P < 0.01$ by $t$ test; $n = 3$ for each group. (C) K68 and K122 mutants of human SOD2 (glutamine substitutions and arginine substitutions) were overexpressed and purified from HEK293T cells, and relative SOD2 activity was measured with WST assay. $^{**}P < 0.01$ by $t$ test compared to control group (wt). $\#\#P < 0.01$ by $t$ test compared to K68Q group; $n = 3$ for each group.

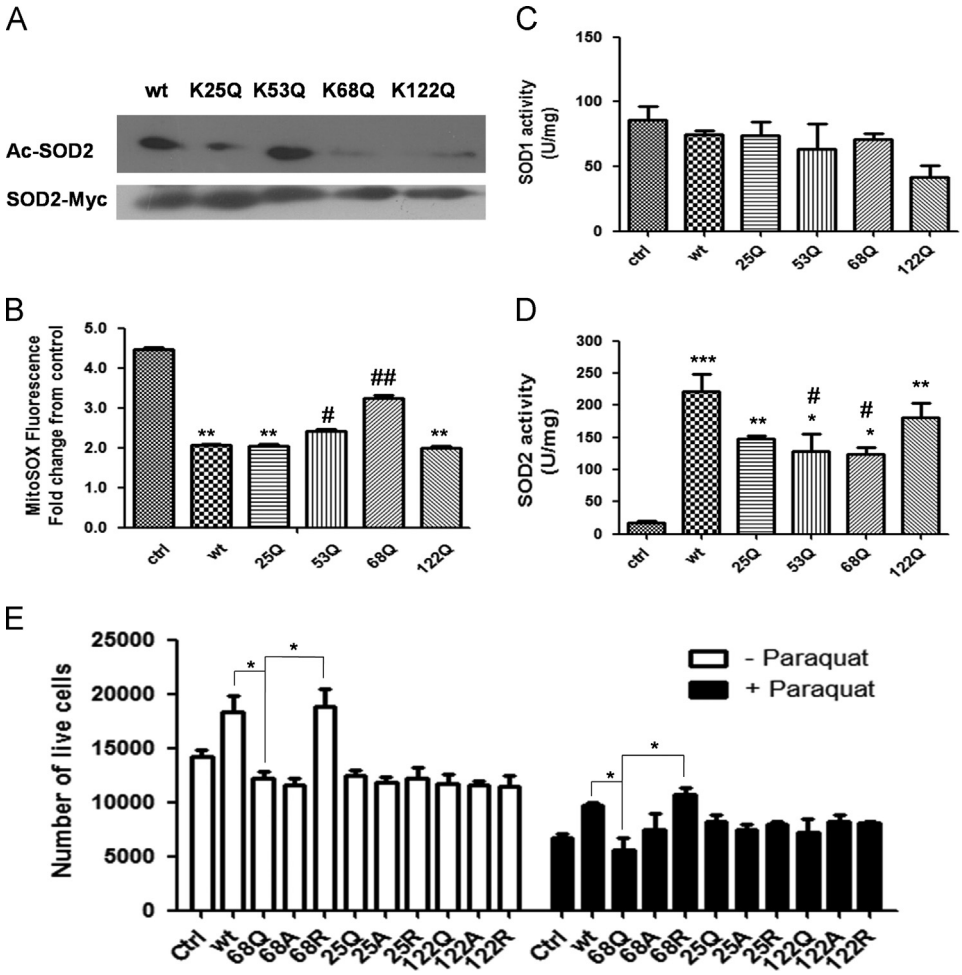


**Fig. 3.** Cellular SOD activities and cell survival numbers upon paraquat treatment were altered by mutation of SOD2 acetylated lysine residues. (A) Total acetylation of all SOD2 mutants was detected by antibody against acetyllysine and total expression level of SOD2–c-myc was detected by c-myc antibody. (B) Mutant cDNAs with glutamine substitutions of each acetylation site of SOD2 were transfected into HEK293T and the mitochondrial superoxide level was measured by addition of MitoSOX (5 μM) to the cells. The control group is the HEK293T cells transfected with the pCMV6-Myc-DDK empty vector. $^{**}P < 0.01$ by $t$ test compared to control group (ctrl). $\#P < 0.05$ by $t$ test compared to wt group, $\#\#P < 0.01$ by $t$ test compared to wt group; $n = 3$ for each group. (C) Assay of SOD1 activity in cellular homogenates overexpressing wild-type and glutamine mutants of the lysines. (D) Measurement of SOD2 activity of cell homogenates overexpressing wild-type and glutamine mutants of the lysine residues. $^{*}P < 0.05$ by $t$ test compared to control group (ctrl). $^{**}P < 0.01$ by $t$ test compared to ctrl. $^{***}P < 0.001$ by $t$ test compared to ctrl. $\#P < 0.05$ by $t$ test compared to wt group; $n = 3$ for each group. (E) 250,000 cells were incubated with 200 μM paraquat for 48 h. Remaining adherent cells were trypsinized and counted using a cell counter. $^{*}P < 0.05$ by $t$ test; $n = 3$ for each group.

mutants compared with that in the control group. The overexpressing K68Q mutant exhibited SOD2 activity lower than that of the wild-type group, in accordance with the MitoSOX data. However, no significant difference in SOD2 activity was found in cell homogenates containing K25Q and K122Q compared with the wild-type group (Fig. 3D). The above results give us some preliminary hints that K68 may have some unique properties among the different lysine sites.

To determine whether the mutations of acetylated lysine residues can cause the physiological changes in the cells, we performed a cell survival assay to compare their sensitivity to paraquat in HEK293T cells overexpressing wild-type and lysine mutants. Overall, the overexpression of the wild-type and lysine mutants of SOD2 could increase the number of live cells compared with the control group when they were treated with 200 μM paraquat for 48 h. The cells overexpressing K68R SOD2 resulted in a significantly higher number of live cells compared to those overexpressing K68Q and K68A with or without paraquat stimulation. The overexpression of the K25 and K122 mutants decreased the numbers of live cells compared with that in the wild-type group. K68Q overexpression significantly resulted in the lowest number of live cells among all groups, including the wild-type cells treated with paraquat (Fig. 3E). Thus, K68 mutation significantly influenced the survival rate of HEK293T cells. All the SOD2 mutants were overexpressed in HEK293T cells, and their SOD2 activities were measured with both MitoSOX staining and SOD activity test (Figs. 4A–4I). A previous study reported that arginine substitution in K122 increased SOD2 activity. However, we were unable to observe that the K122R mutant resulted in the SOD2 activity higher than that of the wild-type on the basis of the MitoSOX data and SOD2 activity results measured in cell lysates (Figs. 4D and 4F). The SOD2 activity was not increased by arginine substitution but decreased in K68A compared with that in the other two mutants (Figs. 4A and 4C), similar to that observed by Chen et al. [30]. The result of SOD activity measurement also showed that the K68A mutation significantly decreased the SOD1 and SOD2 activities in cell lysates, which may explain why K68A can increase the superoxide levels in the mitochondria. Therefore, K68 may not only function as an acetylation site but also possibly affect both the SOD1 and the SOD2 activity through other mechanisms, such as methylation of K68, as revealed by Sarsour et al. [18]. Consistent with these findings, our MS results also indicated that K68 was methylated under physiological conditions in *E. coli* (Table 1). Nevertheless, the reason K68A resulted in the lowest SOD1 activity among all the K68 mutants remains ambiguous. In the K122 mutant, the three types of substitution led to the diminution of SOD1 and SOD2 activities as indicated by the MitoSOX data and SOD activity results (Figs. 4D–4F). K122R exhibited slightly higher activity than K122Q in HEK293T, but without statistical significance (Fig. 4D; $n = 3, P = 0.0665$). This is similar to the results obtained in MEF cells reported by Tao et al. [29]. In addition, no differences in SOD2 activity were observed between the glutamine and the arginine substitutions of the nonacetylated K25 (Figs. 4G–4I). Hence, the substitutions of the nonacetylation site would not alter the SOD2 activity. Based on these results, it is highly probable that K68, among the investigated lysine sites, has a dominant role in regulating the activity of SOD2 by (de)acetylation.

### 3.3. K68 mutations decreased SOD2 activity in an antimycin A-induced superoxide elevation model and a SOD2 mimic acted on SOD2K68 acetylation

Given that K68 seems to be a highly important acetylation site and that K68A significantly decreased SOD2 activity in HEK293T cells, we further examined the ability of K68 mutants to scavenge ROS in the mitochondria. We added antimycin A, an antibiotic that can block the respiratory chain to induce superoxide generation in mitochondria, and detected the superoxide level with respect to various K68 mutants. The results revealed that all K68 mutants had activity lower than that of the wild-type in scavenging the superoxide in the antimycin A-induced superoxide elevation model (Fig. 5A). Antimycin A caused an approximately 1.6-fold increase in the mitochondrial superoxide level in wtSOD2-containing HEK293T, and the elevation of the superoxide was intensified with glutamine substitution and peaked with alanine substitution. We also measured SOD activity of the cellular homogenates of the cells upon antimycin A treatment. The results showed that antimycin A treatment decreased SOD2 activity but promoted SOD1 activity (Fig. 5A). The suppression of SOD2 activity of the wtSOD2-containing cell lysates was more obvious than that of the K68 mutant. The SOD1 activity was significantly increased in K68R-containing cell lysates but was not changed in K68Q- and K68A-containing lysates treated with antimycin A. Moreover, arginine substitution in K68 showed an increase in the MitoSOX data by 1.4-fold but decreased the SOD2 activity in lysates of cells treated with antimycin A (Fig. 5A). Thus, K68R can repress the increased superoxide level more effectively than wtSOD2.

We measured the effect of MnTM-4-PyP on SOD2 activity in scavenging the ROS level in the mitochondria. It can be calculated that compared to the control group, overexpression of wild-type SOD2 could lead to a twofold increase in SOD2 activity and a 40% decrease in MitoSOX level in lysates (Fig. 5B). This mimic did not affect the superoxide level in cells harboring wtSOD2 but altered the superoxide level in the cells harboring the SOD2 K68 mutant (Fig. 5B). We further tested the SOD activity of cellular lysates of cells treated with and without 30 μM MnTM-4-PyP (Fig. 5B). The addition of MnTM-4-PyP elevated the SOD2 activity in lysates overexpressing wtSOD2 and K68 mutant. Moreover, the increase in SOD2 activity was higher in the K68 mutant than in the wild-type. The overexpression system of wild-type SOD2 and SOD2K68R also exhibited decreased SOD1 activity upon MnTM-4-PyP treatment. Therefore, the mechanism of the function of the mimic seems to be K68-dependent. Addition of mimic was suggested to significantly decrease the superoxide level in the mitochondria of K68 mutants. Thus, SOD2 mimic was thought to restore the increased ROS induced by the K68 mutation. Curtis et al. [38] reported that SOD2 overexpression resulted in a declined metabolic rate and that the balance of deacetylation/acetylation shifted to the deacetylation side. Hence, it can be inferred that MnTM-4-PyP affects the endogenous SOD2 activity through deacetylation of K68, particularly when the cells are in the high-rate metabolic state, given that the activity of the wild-type SOD2 is not influenced by the mimic because of the low metabolism rate along with the overexpression of SOD2.

In our recent study with one of the SOD2 mimics, namely, MnTM-4-PyP, we found that this mimic lowered the acetylation level of SOD2 in primary cortical neurons. We also detected the effects of MnTM-4-PyP on the acetylation of K68 of SOD2 in the antimycin A-induced stress model of HEK293T cells (Fig. 5C). We quantitated the band densities of SOD2K68Ac and p53 from three independent experiments. Antimycin A treatment increased the K68 acetylation level of SOD2, whereas MnTM-4-PyP decreased the acetylation level of K68. However, the SIRT3 expression level remained constant during the MnTM-4-PyP treatment. Surprisingly, the expression of p53 was also induced by antimycin A and further intensified when MnTM-4-PyP was added (Fig. 5C). Thus, this observation made us wonder whether the increased p53 level was related to the cellular level of K68 acetylation of the SOD2. The cellular SOD2–p53 interaction will be studied later.

### 3.4. K68 mutations altered the structure and the electrostatic potential of SOD2

We further studied how K68 affects SOD2 activity from three respects, namely, the changes in SOD2 structure, the stability of the SOD2 tetramer, and the electrostatic potential of the SOD2 enzyme caused by K68 mutation. To investigate the influence of K68

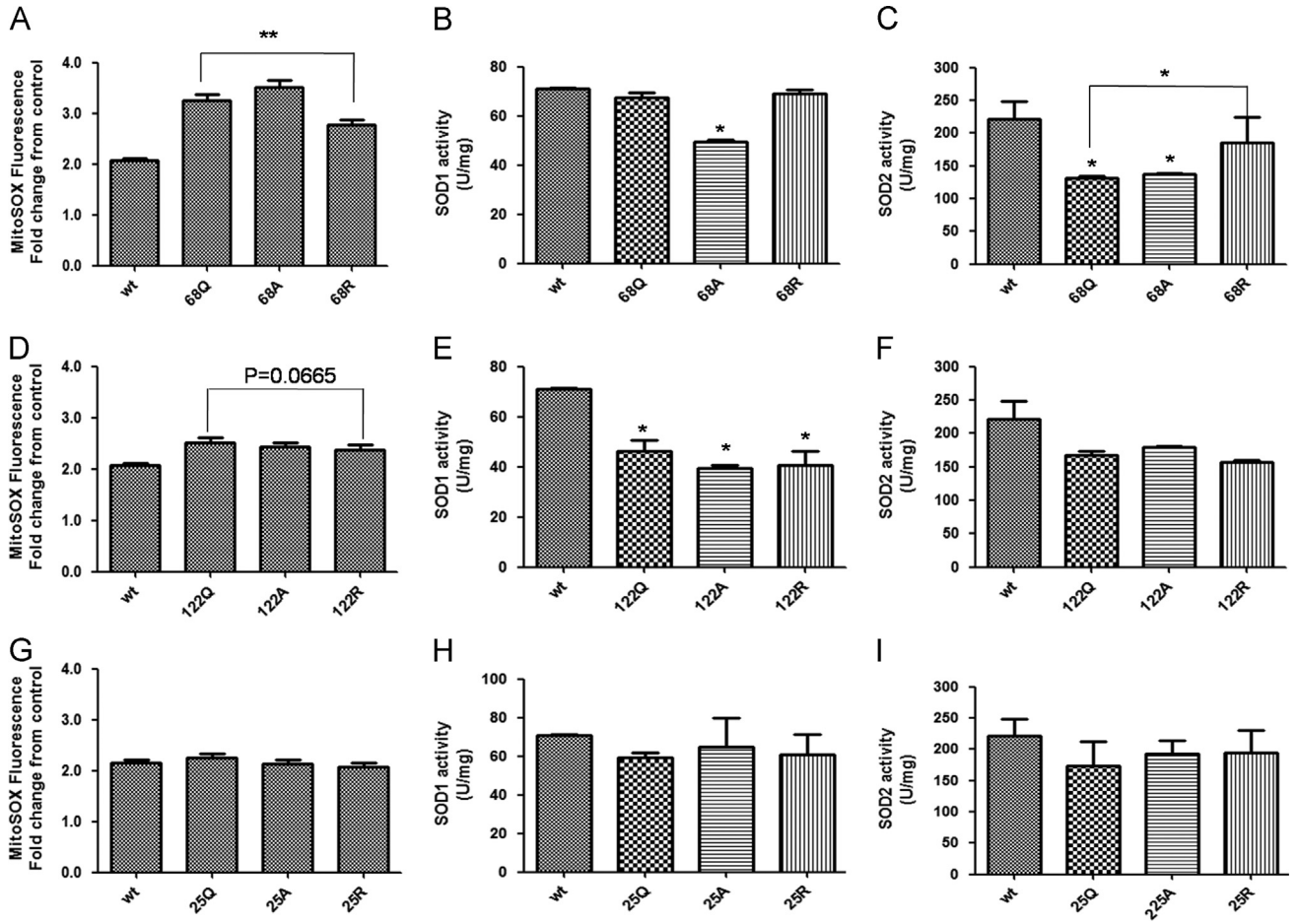


**Fig. 4.** SOD1 and SOD2 activities were affected by glutamine, alanine, and arginine mutations of K68, K122, and K25. The mitochondrial superoxide level of HEK293T cells overexpressing all three substitutions (glutamine, alanine, and arginine) of (A) K68, (D) K122, and (G) K25 of SOD2 were measured. K68 exhibited acetylation-dependent activity which was significant, but not K122 and K25. Data are presented as the average ± SD. $^{**}P < 0.01$ by $t$ test; $n = 3$ for each group. SOD1 and SOD2 activities were tested in HEK293T cells overexpressing (B and C) K68, (E and F) K122, and (H and I) K25 using cell lysates. $^{*}P < 0.05$ by $t$ test; $n = 3$ for each group.

mutation on SOD2 structure, we performed a molecular dynamics simulation based on human SOD2 (PDB 2ADQ) with the Amber11 software. During simulation, the ff99SB, Gaff, and TIP3P force fields were used for protein, Mn, and water, respectively; the simulation defined a three-site rigid water molecule with charges and Lennard–Jones parameters assigned to each of the three atoms. This simulation had a length of 10 ns. The superposition of K68A and the simulation structures of wtSOD2 revealed that the overall conformation of SOD2 was minimally perturbed by the alanine substitution of K68 (Fig. 6A). However, K68A resulted in a significant change in the α-helix constituted by residues 185–192 (red circle in Fig. 6A), which contains the coordinated H187. As shown in Fig. 6A, K68 is located in the middle of the first N-terminal helical hairpin domain responsible for coordinating Mn(III). The first and second N-terminal α-helices display only a slight difference, but a large change is observed in the entire helix that contains residues 185–192. This helix turned out to be loosened because of the alanine substitution of K68, thus extending the distance between H187 and the Mn in the catalytic center, whereas the N-terminal helix that contains K68 is minimally perturbed. Meanwhile, two lysine residues, namely, K25 and K53, which are not too far away from the active site, also showed significant conformational changes between the K68A and the wild-type simulations (Fig. 6B). In the model explored by Zhu et al. [37], the lysine residues of SOD2 probably form a positive cluster responsible for attracting the negatively charged superoxide molecules into the active center of SOD2. The conformation of the electrostatic funnel was altered and thus the SOD2 catalytic activity was changed. We also performed additional molecular dynamics simulations of K122Q and K53Q to determine how other acetylation sites influence the SOD2 structure. The results of these two lysine mutants (Supplementary Fig. 2) showed no changes in their structures relative to the structure of wtSOD2. The conformations of the four active-site residues (H50, H98, D183, and H187) located in the active center of their structures were similar to those in the wild-type structure. Thus, K68 is also a stereochemically sensitive site, whose acetylation may affect SOD activity via the alteration of active-site conformation. The total electrostatic potential surface of SOD2 was also displayed (Fig. 7) to study the total charge alteration of SOD2 because of the alanine substitution of K68. The charge of the region surrounding K68 evidently was reversed because of this mutation. Moreover, the charge distribution of the SOD2 active center also differed extensively, with a big shift from the negative to the positive state (as indicated by the box in Fig. 7). The four active-site residues, H50, H98, D183, and H187, are indicated in the enlarged box region in Fig. 7. It was astonishing that K68A displayed such a big difference, whereas K68Q did not (data not shown). We speculated that the difference in molecular dynamics between K68Q and K68A was due to the stereochemically smaller size of alanine compared to glutamine as well as to their different charges. The K68A mutation changed the overall conformation of the corresponding lysine residue, whose charge determines the total enzymatic activity. The molecular mechanism of this phenomenon must be elucidated in future studies.

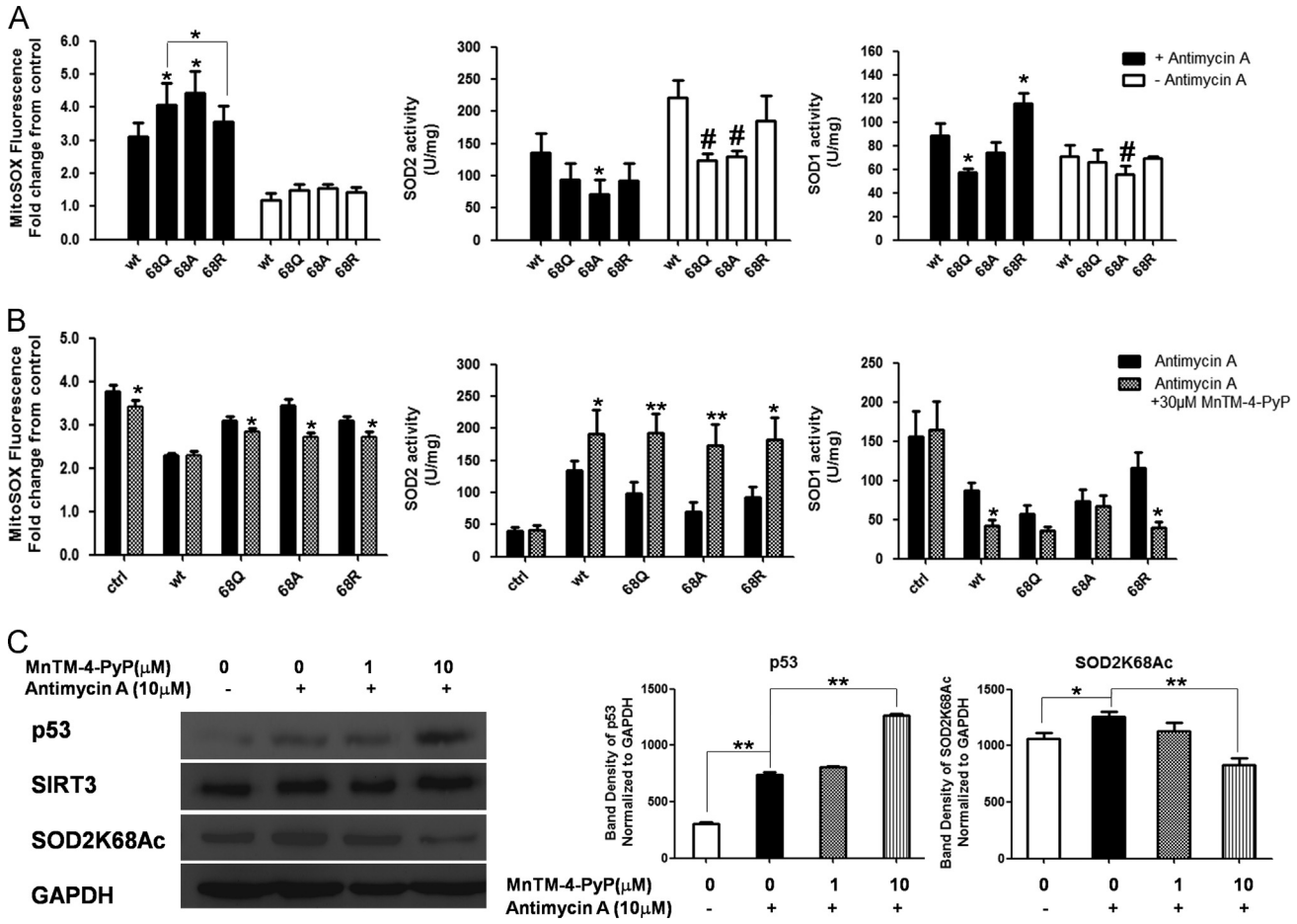


**Fig. 5.** SOD2 regulates cellular ROS level via K68 deacetylation. (A) WtSOD2 and K68Q, K68A, and K68R mutants of SOD2 were overexpressed in HEK293T cells and mitochondrial ROS level was elevated by stimulation with 50 μM antimycin A for 1 h. The ROS levels with or without the addition of antimycin A were determined by MitoSOX staining. SOD1 and SOD2 activities were measured with WST-1 assay. $^{*}P < 0.05$ by $t$ test compared to control group (wt) in antimycin A-treatment groups. $\#P < 0.05$ by $t$ test compared to wt group treated without antimycin A; $n = 3$ for each group. (B) Mitochondrial superoxide was measured with MitoSOX with or without MnTM-4-PyP treatment (30 μM) in an antimycin A-induced superoxide elevation model in control cells (ctrl) and cells harboring wtSOD2 or K68 mutants. The control group is the HEK293T cells transfected with pCMV6-Myc-DDK empty vector. Corresponding SOD1 and SOD2 activities of each group were measured. $^{*}P < 0.05$ by $t$ test between groups with and without MnTM-4-PyP treatment. $^{**}P < 0.01$ by $t$ test between groups with and without MnTM-4-PyP treatment; $n = 3$ for each group. (C) Western blot shows that MnTM-4-PyP treatment decreased K68 acetylation of SOD2 and increased p53 expression in antimycin A-induced model. Density of bands was quantitated using ImageJ software. $^{*}P < 0.05$ by $t$ test. $^{**}P < 0.01$ by $t$ test; $n = 3$ for each group.

### 3.5. The mutations of the SOD2 acetylation sites affected the tetramer stability and protein–protein interactions of SOD2 in HEK293T

In its native state in human cells, SOD2 forms a homotetramer, the active form, to fulfill its role in defending the cells from the attack of superoxides. Hence, we speculated that the substitution of one amino acid might cause the partial charge difference of SOD2 and induce the change in the entire stability of the tetramer. To further assess how the aforementioned lysine mutations contribute to the tetrameric conformation of SOD2 protein, we compared the amount of tetramer to that of the monomer of each mutant. We transfected the cells with wt or mutant SOD2 plasmids and resolved the cell lysates on both native and denatured gels. The native PAGE software was used to detect the native SOD2 tetramer; meanwhile, the SDS–PAGE software was used to reflect the amount of monomer. The tetramer level was calculated by normalizing the tetramer protein levels on the native gel to the expression levels of the monomers detected in the denatured gels. The results indicated that the overall tetramer level of K122 was lower than that of K68 (Fig. 8A). Interestingly, for both K68 and K122, the arginine substitutions resulted in tetramer protein levels higher than those of the alanine and glutamine substitutions, given that the total expression level of SOD2 of all the mutants remained the same in the SDS–PAGE. As an additional note, bands of possible heterotetramers were not observed on the native PAGE gel, because either there were not enough of them to be detected or the different bands were not resolvable owing to the complexity of protein behavior in native PAGE. These results revealed that the mutations of the acetylated lysine residues could affect the cellular level of SOD2 tetramer, indicating that these lysine residues may be involved in the formation and maintenance of the SOD2 tetramer.

Acetylated proteins are widely connected in an intensive protein–protein interaction network, and acetylation exists in large macromolecular complexes. K122 is located near the B2–B3 loop, which is involved in the protein–protein interaction because of the antiparallel orientation of the N-terminal helices [39]. Hence, K122 possibly participates in the assembly of SOD2 tetramers or in the interactions between SOD2 and other proteins. Robbins and Zhao [40] reported that SOD2 interacts with p53 in the mitochondria, and SIRT3 precisely deacetylates K122 of SOD2 [29,30]. On the basis of the findings shown in Fig. 5C, we performed coimmunoprecipitation to detect whether the protein interaction level was altered because of lysine mutations in HEK293T cells. Coimmunoprecipitation was performed on SOD2 with c-myc antibody, whereas immunoblot analysis was conducted with p53 and SIRT3 antibodies. The results

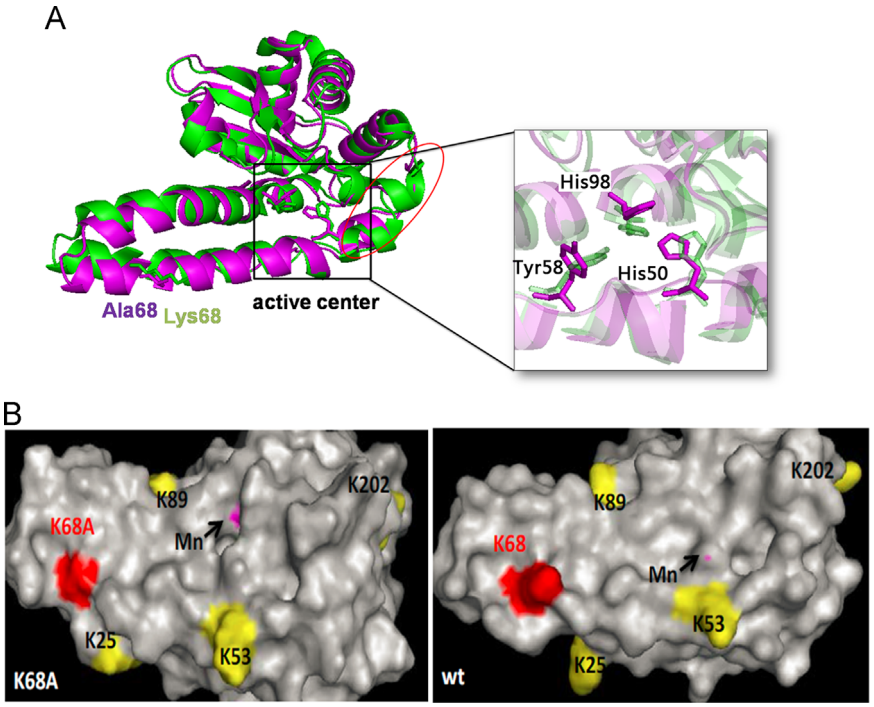


**Fig. 6.** Conformational change in SOD2 active center and the structural alteration around acetylation sites induced by K68 mutation. (A) Molecular simulations were carried out with Amber11 and the superposition of the generated K68A (purple) and wtSOD2 (green) structures is shown. The active center with key residues around manganese is zoomed (inset). The red circle indicates the significant change in the helix constituted by residues 185–192. (B) The surface of the simulated structure of K68A and wtSOD2. Residue 68 is marked red and the reported acetylation sites are marked yellow. The exposure of the ion center Mn was altered by K68 mutation. The images were visualized with PyMOL.

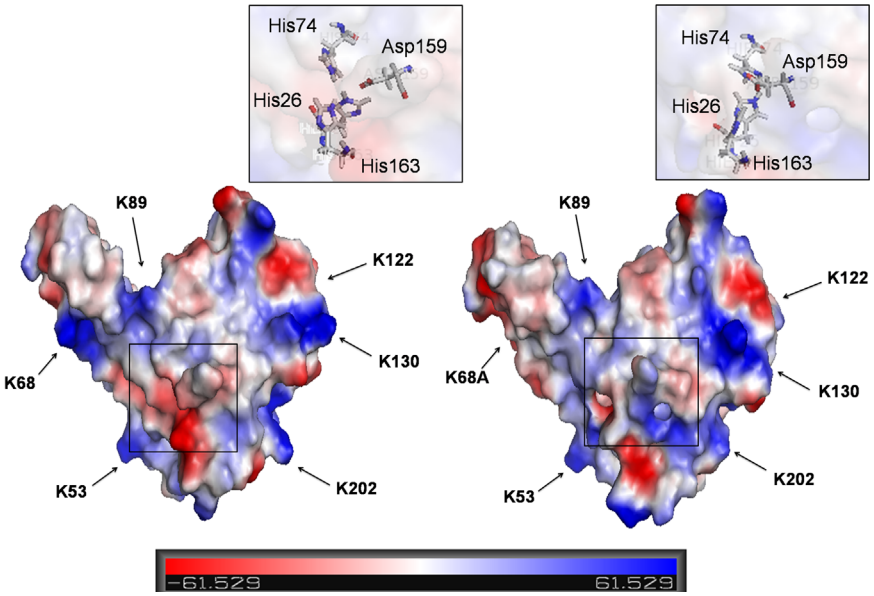


**Fig. 7.** The electrostatic potential on the solvent-accessible surfaces of wtSOD2 and K68A mutant (simulated structure with Amber11) is shown. All the lysine residues indicated by arrows present positive charge (blue) except the K68A mutation site, which displays a negative charge (red). Active sites are identified in the enlarged boxes above the two surfaces. The images were visualized with PyMOL.

(Fig. 8B) indicated an alteration in accordance with the general trend of all the aforementioned mutants in SDS–PAGE. Compared with the K68 and the wild-type mutants, the K122 mutants exhibited a significant decrease in the interaction between SOD2 and p53 and a nonsignificant decrease in the SIRT3–SOD2 interaction, suggesting that K122 may be a part of the factors involved in the mediation of interactions between p53 and SOD2.

Considering our results and those of previous studies, we propose a new explanation with regard to the effects of K68 and K122 on SOD2 activity (Fig. 9). The acetylation of these two lysine residues alters the local charges of the SOD2 protein and decreases its ability to attract superoxide molecules. Acetylation also complicates the transfer and movement of superoxide molecules through the SOD2 protein (superoxide marked yellow in Fig. 9). In addition, mutations of these acetylation sites may negatively affect the assembly and stability of the SOD2 tetramer, thereby downregulating SOD2 activity by loosening the tetramer structure of SOD2. K68 particularly influences the charge distribution of

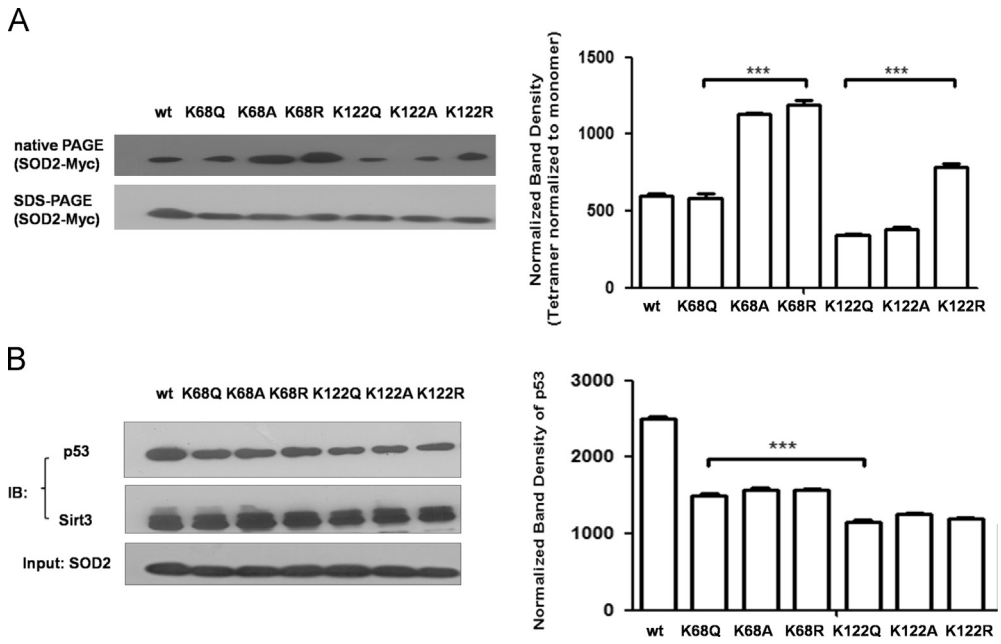


**Fig. 8.** Mutations of SOD2 acetylation sites affect the tetramer stability and protein–protein interactions in HEK293T. (A) Protein expression of all SOD2 mutants was measured by Western blot with c-myc antibody. The bands on native PAGE were normalized to SOD2–myc expression by SDS–PAGE. $^{***}P < 0.001$ by one-way ANOVA, $n = 3$. (B) Coimmunoprecipitation of SOD2 mutants in HEK293T cells. The input was detected with antibody against SOD2 and the precipitated proteins were detected with p53 and SIRT3 antibodies. Normalized p53 expression was subjected to statistical analysis. $^{***}P < 0.001$ by one-way ANOVA, $n = 3$.

SOD2. Moreover, the mutations of these acetylated lysine residues could attenuate the interaction between p53 and SOD2, in which K122 is more likely to be involved.

## 4. Discussion

Superoxide is the main ROS that causes oxidative damage to organisms and also functions as a signal molecule. The negative correlation between mitochondrial superoxide molecules and life span has been validated in *Caenorhabditis elegans* [41]. Moreover, the scavenging activity of SOD2 plays a significant role in maintaining the mitochondrial and cellular superoxide levels. It is well known that the expression and activity of SOD2 could be modulated by many physiological stimuli, including lipopolysaccharide, cytokines, and ionizing radiation [42,43]. However, few studies have focused on how acetylation functions in these processes. It has been reported that tumor necrosis factor could induce a 10-fold increase in SOD2 but no results have shown how acetylation is changed in this situation. Tao et al. [29] validated that the elevated SOD2 activity was consistent with decreased lysine acetylation in mice subjected to ionizing radiation. We previously confirmed the protective effect of the SOD2 mimic MnTM-4-PyP against $H_2O_2$-induced oxidative injury on primary cultured rat cortical neurons [44]. Moreover, the SOD2 mimic was found to promote SOD2 deacetylation in neurons. Nevertheless, the functions of SOD2 deacetylation and the location of the main acetylation site(s) remain unknown.

To our knowledge, we are the first to have achieved the overall SOD2 acetylation in vitro using the chemical acetylation method in this study. Meanwhile, we developed a method for measuring the activity of SOD2 mutants in HEK293T cells and identified K68 as the key residue that regulates SOD2's activity by (de)acetylation, because only the K68 site exhibited a clear difference in SOD2 enzymatic activities, MitoSOX fluorescence intensities and cell survival rates among the three mutants, especially with the R mutant's (deacetylated lysine mimic) activity significantly higher than that of the Q mutant (acetylated lysine mimic). By contrast, the data of K25 and K122, for example, did not show significant

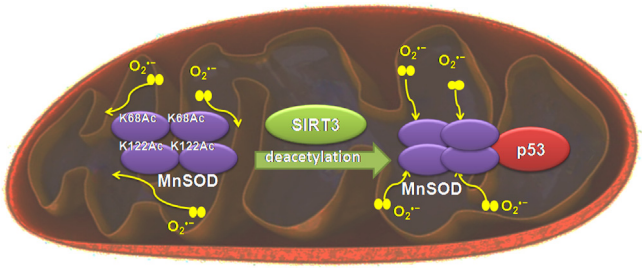


**Fig. 9.** Scheme: the regulation of activity and tetramer stability of SOD2 via K68 acetylation. In this model we elucidate the mechanisms underlying the decrease in superoxide-scavenging activity of SOD2 caused by acetylation. The acetylation of K68 and K122 in SOD2 would result in the loosening of the SOD2 tetramer and alter the SOD2 structure and electrostatic potential, thus leading to electric repulsion between the superoxide and the SOD2 surface. Meanwhile the mutations of acetylated lysine residues would affect p53–SOD2 interaction in mitochondria. And SIRT3 would promote SOD2 activity by deacetylating K68 and K122 and restore these impacts brought by SOD2 acetylation.

differences among the three mutants, which indicates a lack of sensitivity of enzymatic activity to the electrostatics at these sites. We adopted computational approaches to study the structure and electrostatic potential of the SOD2 K68A mutant. Based on the results, we proposed that the acetylation of K68 would induce a conformational shift of the coordinated sites in the active center, including H50, H98, and H187, which are the key ligands to form coordination bonds with Mn. The distance between Mn and these coordinating residues increased in the K68A mutant, which theoretically would lead to an elevation of the Mn redox potential. The exact value of the redox potential can be difficult to obtain, but qualitatively the deviation of Mn redox potential from an optimal value would probably detract from the catalytic efficiency of SOD2. In addition, Y34, which is located in the second coordinated shell of SOD2 and whose conformation is changed to a large extent because of the K68 mutation, is vital in the $H_2O_2$ inhibition of the SOD2 model [45]. Furthermore, Jason Porta et al. analyzed the structure of peroxide-soaked SOD2 and found that the peroxide would cause the shift of the Y34 when peroxide was trapped in the

active center of the SOD2 [46]. Hence, whether acetylation of K68 plays a role in the peroxide-bound SOD2 remains to be studied. Furthermore, the K68A mutation induced the overall electrostatic change in which the positively charged region around the K68 and the active center shifted to a negative charge, decreasing the ability of the mutation to attract superoxide molecules. We then investigated the effects of the mutations of the acetylation sites and unexpectedly found that acetylation at this site affected tetramer stability and protein–protein interaction of SOD2 in human cells.

Interestingly, we revealed that K122 mutants did not change the SOD2 activity too much compared with K68 mutants (Figs. 3B and 3D). To date, none of the MS results have identified K122 as the acetylation site in human cells. Only Tao et al. [29] indicated that K122 was a conserved acetylation site in mice, and its acetylation significantly decreased the SOD2 activity. However, in our study, we detected K122 acetylation only in chemically acetylated SOD2 through MS (Supplementary Table 2) and did not find that K122 could remarkably affect the SOD2 activity (Figs. 4A and 4B). We reasoned that this observation may be caused by the location of K122 on the SOD2 structure. K122 is located in a region that is far away from the active center, and this residue extends out from the SOD2 surface, which indicates that, being more accessible than other sites, it may be easier for this lysine residue to undergo deacetylation too quickly for us to detect through MS. However, the precise mechanism by which K122 acetylation affects SOD2 activity still remains unclear.

MitoSOX red is a probe widely used in the detection of superoxide in mitochondria [30,18], although its reliability is still questioned nowadays [47]. In a simple chemical system, MitoSOX could react with superoxide to form a red fluorescent product, mito-2-hydroxyethidium, which is used to detect superoxide. However, in a complex biological system, other oxidative products can be generated in this reaction, which may disturb the measurement of superoxide. The effects caused by autoxidation of MitoSOX could be decreased by normalizing them to the control group in the experiment. The overexpression of SOD2 may also prevent oxidation of MitoSOX by other oxidants. In this paper, we combined the MitoSOX data and the SOD activity of lysates to compare the superoxide-scavenging capabilities of wtSOD2 and various mutants. The SOD2 activity levels in cell homogenates were consistent with the MitoSOX results. The overexpression of K68A could lead to the highest level of MitoSOX as well as the lowest SOD2 activity. The SOD2 activity was not increased by arginine substitution but significantly decreased in K68A compared with that in the other two mutants (Fig. 3C). Although K68 mainly functions as an acetylation site, this mutation may also affect the SOD2 activity through other mechanisms, including K68 methylation, as revealed by Sarsour et al. [18]. We have also detected the methylation level of SOD2 in HEK293T cells treated with or without MnTM-4-PyP through MS and detected the monomethylation of K68 with MnTM-4-PyP (Supplementary Fig. 3). Hence, a cross talk between acetylation and methylation seems to exist in K68 to mediate the SOD2 activation. This interplay between two different modifications of the same residue may have the fundamental implications for understanding how the enzymes are activated. In the study on the effects of MnTM-4-PyP (Fig. 5B), the MitoSOX data are different from the SOD2 activity results. The results shown in Fig. 5B indicate that MnTM-4-PyP did not cause much change in mitochondrial superoxide level in wt cells but significantly lowered the mitochondrial superoxide level in K68 mutant cells. This finding could be attributed to the decreased SOD1 activity induced by MnTM-4-PyP that may offset the increased SOD2 activity after treatment with MnTM-4-PyP. These mechanisms generally function to maintain the constant mitochondrial superoxide level after treatment with SOD2 mimic.

In the physiological state, SOD2 monomers assemble to form tetramers. In our research, acetylation changed the charges in SOD2 and significantly affected the tetramerization of SOD2 monomers. The denatured K68 mutant formed three bands in the SDS–PAGE in vitro, whereas wtSOD2 was depolymerized after boiling (Supplementary Fig. 4). The underlying mechanism may be that the lysine acetylation will diminish the positive charge, thereby decreasing the electrostatic repulsion between monomers, making the tetramer stable. According to Marius Schmidt et al., the four subunits of SOD2 in *Propionibacterium shermanii* are held together by H-bonds between residues of the two distorted helical turns, following one sheet and the equivalent area in the other monomer [38,48]. One H-bond also exists between Q122, located in the loop from H4 to B1, and D64, located in the H2 of the other monomer. For K122 in human cells, similar bonds possibly exist and the specific localization of K122 may facilitate the protein–protein interactions at this site. Nevertheless, the possibility that nonacetylated lysine K25 can also affect the overall acetylation level of SOD2 through glutamine substitution seems to be odd (Fig. 3A). One possible explanation is that amino acids 1–24 of the human SOD2 constitute the mitochondrial localization sequence; thus, K25 becomes the real N-terminal amino acid whose mutation may affect the recognition between the anti-acetyllysine antibody and other acetyllysine residues.

The endogenous SOD2 may encounter many proteins to fulfill its role in mitochondria, thus forming a complex redox network to regulate cellular superoxide level [49]. It has been reported that in the mitochondrion SOD2 may function together with p53 to achieve better superoxide-scavenging activity [50]. It has been well known that p53 translocates to mitochondria to maintain mitochondrial genetic stability when cells undergo stress such as UV irradiation [51]. The interaction between SOD2 and p53 in vivo and in vitro was also validated by Zhao and colleagues [40,52,53]. In their study, p53 functions together with SOD2 in the mitochondria to repair mitochondrial DNA under oxidative stress. Bakthavatchalu et al. [52] also found that p53 formed a complex with SOD2 by interacting with the DNA polymerase γ. Nevertheless, the detailed mechanism underlying p53–SOD2 interaction and the exact sites that mediate this interaction remain to be determined. We propose that the acetylation sites of SOD2 are involved in the p53–SOD2 interaction, thus providing a new perspective to study acetylation-dependent SOD2 activity. To the best of our knowledge, this study is the first to investigate the SOD2 acetylation in vitro from the structural aspect and to present detailed discussion of the posttranslational modification. A similar mechanism may be also involved in the regulation of other mitochondrial proteins.

In conclusion, using our SOD2 activity model subjected to acetylation, we identified K68 as the most important acetylation site in SOD2 in human cells, which significantly affects SOD2 activity. Meanwhile, this study described the electrostatic potential and tetrameric stability of SOD2 and proposes that acetylation influences SOD2 activity by affecting the charge distribution and tetramerization of SOD2. This finding may promote further understanding of both SOD2 acetylation sites and the effect of acetylation at these sites on the structure and functions of SOD2. This study has laid a foundation for further study on SOD2 acetylation in diseases and has provided a theoretical basis for the discovery of a novel therapy for oxidative stress- and aging-related diseases in the future.

## Acknowledgments

This work was supported by research grants from the National Natural Science Foundation of China (21371013), Beijing Nova

Program (No. 2010010), and National Key Basic Research Foundation of China (973, No. 2010CB12300).

## Appendix A. Supporting information

Supplementary data associated with this article can be found in the online version at http://dx.doi.org/10.1016/j.freeradbiomed.2015.04.011.

## References


[1] Liu, Y.; Fiskum, G.; Schubert, D. Generation of reactive oxygen species by the mitochondrial electron transport chain. *J. Neurochem.* **80:**780–787; 2002.

[2] Candas, D.; Li, J. J. MnSOD in oxidative stress response-potential regulation via mitochondrial protein influx. *Antioxid. Redox Signaling* **20:**1599–1617; 2014.

[3] Hengartner, M. O. Apoptosis: death cycle and Swiss army knives. *Nature* **391:**441–442; 1998.

[4] Guarente, L. Mitochondria—a nexus for aging, calorie restriction, and sirtuins? *Cell* **132:**171–176; 2008.

[5] Fukui, M.; Choi, H. J.; Zhu, B. T. Mechanism for the protective effect of resveratrol against oxidative stress-induced neuronal death. *Free Radic. Biol. Med.* **49:**800–813; 2010.

[6] Papa, L.; Hahn, M; Marsh, E. L.; Evans, B. S.; Germain, D. SOD2 to SOD1 switch in breast cancer. *J. Biol. Chem.* **289:**5412–5416; 2014.

[7] Boyle, K. E.; Newsom, S. A.; Janssen, R. C.; Lappas, M.; Friedman, J. E. Skeletal muscle SOD2, mitochondrial complex II, and SIRT3 enzyme activities are decreased in maternal obesity during human pregnancy and gestational diabetes mellitus. *J. Clin. Endocrinol. Metab.* **98:**E1601–E1609; 2013.

[8] Cadenas, E.; Davies, K. J. Mitochondrial free radical generation, oxidative stress, and aging. *Free Radic. Biol. Med.* **29:**222–230; 2000.

[9] Sheng, Y.; Abreu, I. A.; Cabelli, D. E.; Maroney, M. J.; Miller, A-F.; Teixeira, M.; Valentine, J. A. Superoxide dismutases and superoxide reductases. *Chem. Rev.* **114:**3854–3918; 2014.

[10] Wang, W.; Fang, H.; Groom, L.; Cheng, A.; Zhang, W.; Liu, J.; Wang, X.; Li, K.; Han, P.; Zheng, M.; et al. Superoxide flashes in single mitochondria. *Cell* **134:**279–290; 2008.

[11] Borgstahl, G. E.; Parge, H. E.; Hickey, M. J.; Johnson, M. J.; Boissinot, M.; Hallewell, R. A.; Lepock, J. R.; Cabelli, D. E.; Tainer, J. A. Human mitochondrial manganese superoxide dismutase polymorphic variant Ile58Thr reduces activity by destabilizing the tetrameric interface. *Biochemistry* **35:**4287–4297; 1996.

[12] Hernandez-Saavedra, D.; Quijano, C.; Demicheli, V.; Souza, J. M.; Radi, R.; McCord, J. M. Thiol-sensitive mutant forms of human SOD2, L60F, and I58T: the role of Cys140. *Free Radic. Biol. Med.* **48:**1202–1210; 2010.

[13] Celotto, A. M.; Liu, Z.; VanDemark, A. P.; Palladino, M. J. A novel Drosophila SOD2 mutant demonstrates a role for mitochondrial ROS in neurodevelopment and disease. *Brain Behav* **2:**424–434; 2012.

[14] Redondo-Horcajo, M.; Romero, N.; Martinez-Acedo, P.; Martinez-Ruiz, A.; Quijano, C.; Lourenco, C. F.; Movilla, N.; Enriquez, J. A.; Rodriguez-Pascual, F.; Rial, E.; et al. Cyclosporine A-induced nitration of tyrosine 34 SOD2 in endothelial cells: role of mitochondrial superoxide. *Cardiovasc. Res.* **87:**356–365; 2010.

[15] Quijano, C.; Romero, N.; Radi, R. Tyrosine nitration by superoxide and nitric oxide fluxes in biological systems: modeling the impact of superoxide dismutase and nitric oxide diffusion. *Free Radic. Biol. Med.* **39:**728–741; 2005.

[16] Ozden, O.; Park, S. H.; Kim, H. S.; Jiang, H.; Coleman, M. C.; Spitz, D. R.; Gius, D Acetylation of SOD2 directs enzymatic activity responding to cellular nutrient status or oxidative stress. *Aging (Albany NY)* **3:**102–107; 2011.

[17] Qiu, X; Brown, K.; Hirschey, M. D.; Verdin, E.; Chen, D. Calorie restriction reduces oxidative stress by SIRT3-mediated SOD2 activation. *Cell Metab.* **12:**662–667; 2010.

[18] Sarsour, E. H.; Kalen, A. L.; Xiao, Z.; Veenstra, T. D.; Chaudhuri, L; Venkataraman, S.; Reigan, P.; Buettner, G. R.; Goswami, P. C. Manganese superoxide dismutase regulates a metabolic switch during the mammalian cell cycle. *Cancer Res.* **72:**3807–3816; 2012.

[19] Candas, D.; Fan, M.; Nantajit, D.; Vaughan, A. T.; Murley, J. S.; Woloschak, G. E.; Grdina, D. J.; Li, J. J. CyclinB1/Cdk1 phosphorylates mitochondrial antioxidant SOD2 in cell adaptive response to radiation stress. *J. Mol. Cell Biol.* **5:**166–175; 2012.

[20] Castellano, I.; Cecere, F.; De Vendittis, A.; Cotugno, R.; Chambery, A.; Di Maro, A.; Michniewicz, A.; Parlato, G.; Masullo, M.; Avvedimento, E. V.; et al. Rat mitochondrial manganese superoxide dismutase: amino acid positions involved in covalent modifications, activity, and heat stability. *Biopolymers* **91:**1215–1226; 2009.

[21] Qian, M-X.; Pang, Y.; Liu; Cui, H.; Haratake, K.; Du, B-Y.; Ji, D-Y.; Wang, G-F.; Zhu, Q-Q.; Song, W.; Yu, Y.; et al. Acetylation-mediated proteasomal degradation of core histones during DNA repair and spermatogenesis. *Cell* **153:**1012–1024; 2013.

[22] Schwer, B. Reversible lysine acetylation controls the activity of the mitochondrial enzyme acetyl-CoA synthetase 2. *Proc. Natl. Acad. Sci. USA* **103:**10224–10229; 2006.

[23] Wagner, G. R.; Payne, R. M. Widespread and enzyme-independent N-acetylation and N-succinylation of proteins in the chemical conditions of the mitochondrial matrix. *J. Biol. Chem.* **288:**29036–29045; 2013.

[24] Choudhary, C.; Kumar, C.; Gnad, F.; Nielsen, M. L.; Rehman, M.; Walther, T. C.; Olsen, J. V.; Mann, M. Lysine acetylation targets protein complexes and co-regulates major cellular functions. *Science* **325:**834–840; 2009.

[25] Kim, S. C.; Sprung, R.; Chen, Y.; Xu, Y.; Ball, H.; Pei, J.; Cheng, T.; Kho, Y.; Xiao, H.; Xiao, L.; et al. Substrate and functional diversity of lysine acetylation revealed by a proteomics survey. *Mol. Cell* **23:**607–618; 2006.

[26] Zhao, S.; Xu, W.; Jiang, W.; Yu, W.; Lin, Y.; Zhang, T.; Yao, J.; Zhou, L.; Zeng, Y.; Li, H.; et al. Regulation of cellular metabolism by protein lysine acetylation. *Science* **327:**1000–1004; 2010.

[27] Xiong, Y.; Guan, K. L. Mechanistic insights into the regulation of metabolic enzymes by acetylation. *J. Cell Biol.* **198:**155–164; 2012.

[28] Lothrop, A. P.; Torres, M. P.; Fuchs, S. M. Deciphering post-translational modification codes. *FEBS Lett.* **587:**1247–1257; 2013.

[29] Tao, R.; Coleman, M. C.; Pennington, J. D.; Ozden, O.; Park, S. H.; Jiang, H.; Kim, H. S.; Flynn, C. R.; Hill, S.; Hayes; McDonald, W.; et al. Sirt3-mediated deacetylation of evolutionarily conserved lysine 122 regulates SOD2 activity in response to stress. *Mol. Cell* **40:**893–904; 2010.

[30] Chen, Y.; Zhang, J.; Lin, Y.; Lei, Q.; Guan, K-L.; Zhao, S.; Xiong, Y. Tumour suppressor SIRT3 deacetylates and activates manganese superoxide dismutase to scavenge ROS. *EMBO Rep.* **12:**534–541; 2011.

[31] Jiang, W.; Wang, S.; Xiao, M.; Lin, Y.; Zhou, L.; Lei, Q.; Xiong, Y.; Guan, K-L.; Zhao, S. Acetylation regulates gluconeogenesis by promoting PEPCK1 degradation via recruiting the UBR5 ubiquitin ligase. *Mol. Cell* **43:**33–44; 2011.

[32] Kim, H-S.; Patel, K.; Muldoon-Jacobs, K.; Bisht, K. S.; Aykin-Burns, N.; Pennington, J. D.; van der Meer, R.; Nguyen, P.; Savage, J.; Owens, K. M.; et al. SIRT3 is a mitochondria-localized tumor suppressor required for maintenance of mitochondrial integrity and metabolism during stress. *Cancer Cell* **17:**41–52; 2010.

[33] Bause, A. S.; Haigis, M. C. SIRT3 regulation of mitochondrial oxidative stress. *Exp. Gerontol.* **48:**634–639; 2013.

[34] Bause, A. S.; Matsui, M. S.; Haigis, M. C. The protein deacetylase SIRT3 prevents oxidative stress-induced keratinocyte differentiation. *J. Biol. Chem.* **288:**36484–36491; 2013.

[35] Chen, I. C.; Chiang, W. F.; Liu, S. Y.; Chen, P. F.; Chiang, H. C. Role of SIRT3 in the regulation of redox balance during oral carcinogenesis. *Mol. Cancer* **12:**68; 2013.

[36] Fridovich, Irwin. Superoxide radical: an endogenous toxicant. *Ann. Rev. Pharmacol. Toxicol.* **23:**239–257; 1983.

[37] Zhu, Y.; Park, S-H.; Ozden, O.; Kim, H. -S.; Jiang, H.; Vassilopoulos, A.; Spitz, D. R.; Gius, D. Exploring the electrostatic repulsion model in the role of Sirt3 in directing SOD2 acetylation status and enzymatic activity. *Free Radic. Biol. Med.* **53:**828–833; 2012.

[38] Curtis, C.; Landis, G. N.; Folk, D.; Wehr, N. B.; Hoe, N.; Waskar, M.; Abdueva, D.; Skvortsov, D.; Ford, D.; Luu, A.; et al. Transcriptional profiling of SOD2-mediated lifespan extension in Drosophila reveals a species-general network of aging and metabolic genes. *Genome Biol.* **8:**R262; 2007.

[39] Schmidt, M.; Meier, B.; Parak, F. X-ray structure of the cambialistic superoxide dismutase from Propionibacterium shermanii active with Fe or Mn. *J. Bioinorg. Chem.* **1:**532–541; 1996.

[40] Robbins, D.; Zhao, Y. Oxidative stress induced by SOD2–p53 interaction: pro- or anti-tumorigenic? *J. Signal Transduct* **2012:**101465; 2012.

[41] Shen, E-Z.; Song, C-Q.; Lin, Y.; Zhang, W-H.; Su, P-F.; Liu, W-Y.; Zhang, P.; Xu, J.; Lin, N.; Zhan, C.; et al. Mitoflash frequency in early adulthood predicts lifespan in Caenorhabditis elegans. *Nature* **508:**128–132; 2014.

[42] Grdina, D. J.; Murley, J. S.; Miller, R. C.; Mauceri, H. J.; Sutton, H. G.; Thirman, M. J.; Li, J. J.; Woloschak, G. E.; Weichselbaum, R. R. A manganese superoxide dismutase (SOD2)-mediated adaptive response. *Radiat. Res.* **179:**115–124; 2013.

[43] Paludo, F. J.; Bristot, I. J.; Alho, C. S.; Gelain, D. P.; Moreira, J. C. Effects of 47C allele (rs4880) of the SOD2 gene in the production of intracellular reactive species in peripheral blood mononuclear cells with and without lipopolysaccharides induction. *Free Radic. Res.* **48:**190–199; 2014.

[44] Huang, H-F.; Guo, F.; Cao, Y-Z.; Shi, W.; Xia, Q. Neuroprotection by manganese superoxide dismutase (SOD2) mimics: antioxidant effect and oxidative stress regulation in acute experimental stroke. *CNS Neurosci. Ther.* **18:**811–818; 2012.

[45] Sheng, Y.; Stich, T. A.; Barnese, K.; Gralla, E. B.; Cascio, D.; Britt, R. D.; Cabelli, D. E.; Valentine, J. S. Comparison of two yeast SOD2s: mitochondrial Saccharomyces cerevisiae versus cytosolic Candida albicans. *J. Am. Chem. Soc.* **133:**20878–20889; 2011.

[46] Porta, J.; Vahedi-Faridi, A.; Borgstahl, G. E. O. Structural analysis of peroxide-soaked MnSOD crystals reveals side-on binding of peroxide to active-site manganese. *J. Mol. Biol.* **399:**377–384; 2010.

[47] Zielonka, J.; Kalyanaraman, B. Hydroethidine- and MitoSOX-derived red fluorescence is not a reliable indicator of intracellular superoxide formation: another inconvenient truth. *Free Radic. Biol. Med.* **48:**983–1001; 2010.

[48] Schmidt, M. Manipulating the coordination number of the ferric iron within the cambialistic superoxide dismutase of Propionibacterium shermanii by changing the pH-value: a crystallographic analysis. *Eur. J. Biochem.* **262:**117–127; 1999.

[49] Tao, R.; Vassilopoulos, A.; Parisiadou, L.; Yan, Y.; Gius, D. Regulation of MnSOD enzymatic activity by Sirt3 connects the mitochondrial acetylome signaling networks to aging and carcinogenesis. *Antioxid. Redox Signaling* **20:**1646–1654; 2014.

[50] Pani, G.; Koch, O. R.; Galeotti, T. The p53–p66shc–manganese superoxide dismutase (SOD2) network: a mitochondrial intrigue to generate reactive oxygen species. *Int. J. Biochem. Cell Biol.* **41:**1002–1005; 2009.
[51] Zhou, B; Liu, X.; Mo, X.; Xue, L.; Darwish, D.; Qiu, W.; Shih, J.; Hwu, E. B.; Luh, F.; Yen, Y. The human ribonucleotide reductase subunit hRRM2 complements p53R2 in response to UV-induced DNA repair in cells with mutant p53. *Cancer Res.* **63:**6583–6594; 2003.
[52] Bakthavatchalu, V.; Dey, S.; Xu, Y.; Noel, T.; Jungsuwadee, P.; Holley, A. K.; Dhar, S. K.; Batinic-Haberle St I.; Clair, D. K. Manganese superoxide dismutase is a mitochondrial fidelity protein that protects Polgamma against UV-induced inactivation. *Oncogene* **31:**2129–2139; 2012.
[53] Zhao, Y.; Chaiswing, L.; Velez, J. M.; Batinic-Haberle, I.; Colburn, N. H.; Oberley St T. D; Clair, D. K. p53 translocation to mitochondria precedes its nuclear translocation and targets mitochondrial oxidative defense protein-manganese superoxide dismutase. *Cancer Res.* **65:**3745–3750; 2005.